

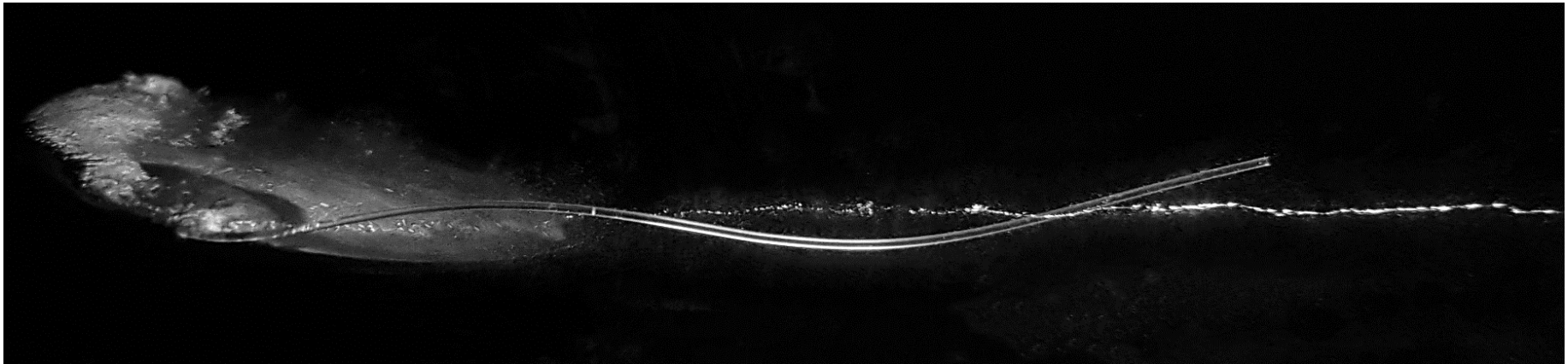
ÉCOLE POLYTECHNIQUE FÉDÉRALE DE LAUSANNE

SGM - 6th & 8th Semester, Fall 2025

CAVITATION AND INTERFACE PHENOMENA

Chapter 5: Vortex Cavitation

5.3: Flow Control for Tip Vortex Cavitation Mitigation



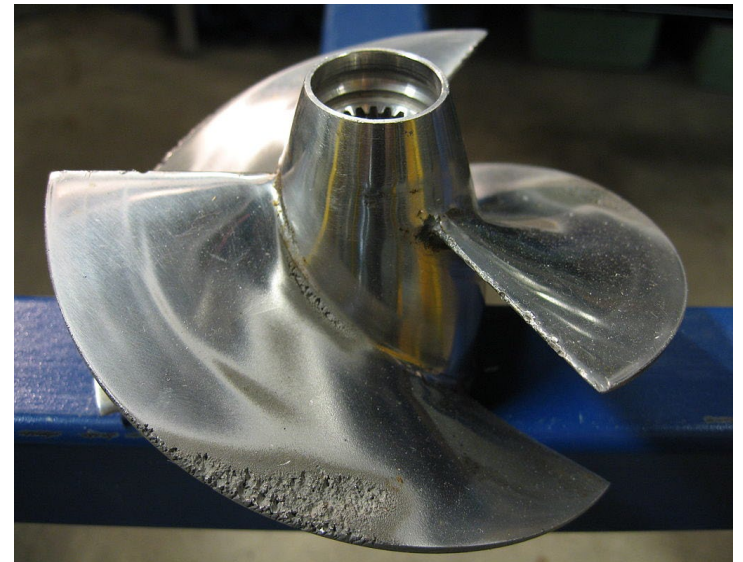
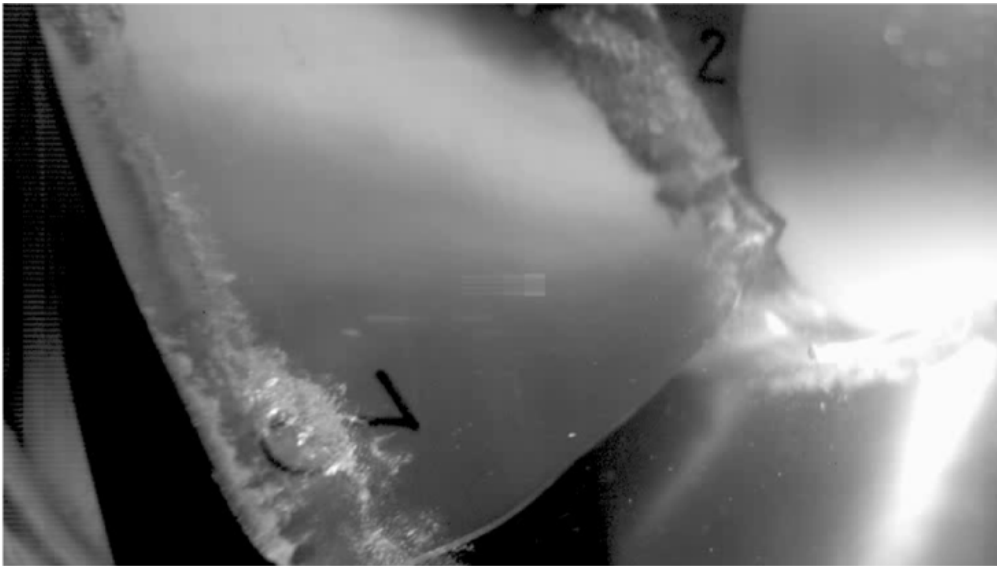
By Dr Ali Amini

Dr Mohamed FARHAT Assistants: A. Sache, Th. Berger

EPFL – Cavitation Research Group, Avenue de Cour 33 bis, 1007 Lausanne

Tip vortex cavitation consequences

- **TVC** may occur in **axial** hydraulic machines
 - Risk of severe erosion in stationary and rotating parts



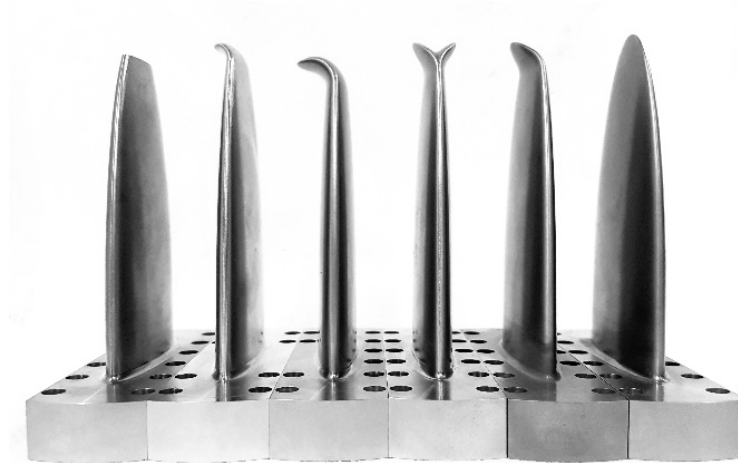
Visualization of TVC in an axial turbine

Erosion of the blade tip in a propeller

TVC Mitigation techniques

- Passive or active injections
 - Water or viscoelastic polymer solutions
- Adding artificial roughness to the tip
- Bulbous tips
- ...

Suppressing Tip Vortex Cavitation by Winglets



Ali Amini, Martino Reclari, Takeshi Sano, Masamichi Iino, and Mohamed Farhat. "Suppressing tip vortex cavitation by winglets." *Experiments in Fluids* 60, no. 11 (2019): 159.

Introduction

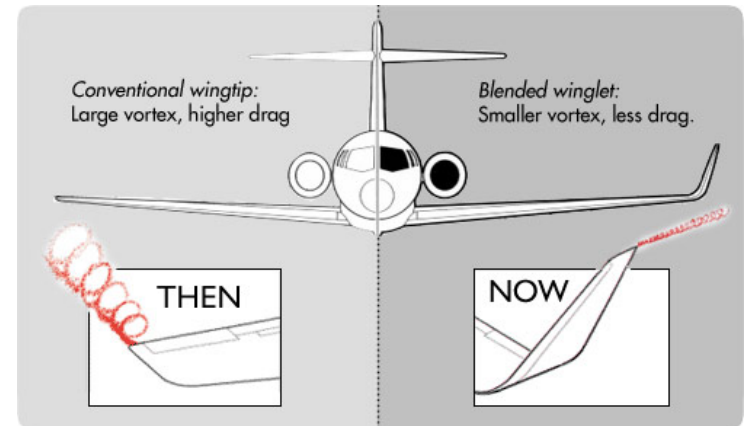
Tip vortices are a source of concern in aeronautics

- Lift-induced drag & flight hazards

✓ A common remedy is appending winglets to wingtips

- Widely used in commercial airplanes
- A large variety of winglets design
- No unique solution exists

- Each winglet has to be carefully designed based on the objectives and constraints.



Introduction

Anti-cavitation lips already exist, but ...

- A survey on **44** projects performed at **LMH** during the last **15 years** revealed that
 - **Only 27%** → **All on the suction side**
 - Usually have simple geometries
- ✓ A step towards **real winglet designs**
- Simple and generic geometries
 - Physical aspects of the flow

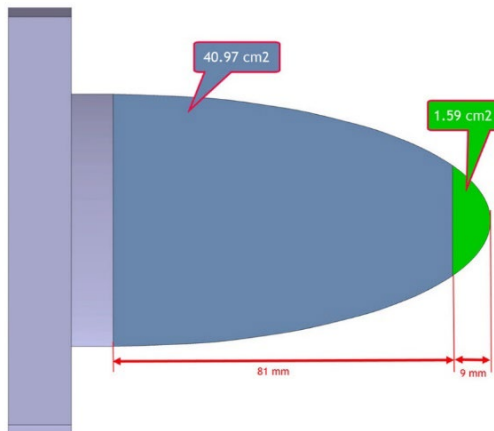
source: www.andritz.com



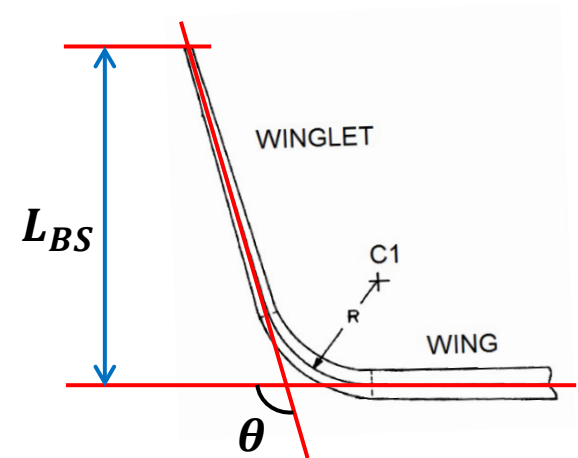
Experimental Setup

The winglets are realized by **non-planar extensions** of the **original** section at various angles

- Design variables: θ & L_{BS}
- Smooth transition of the geometry



The affected area is **max. 3.7%** of the whole lifting surface.



Dihedral angle: $\theta = 0^\circ, \pm 45^\circ, \pm 90^\circ$

Bent section length: $L_{BS} = 0.05S$ & $0.1S$

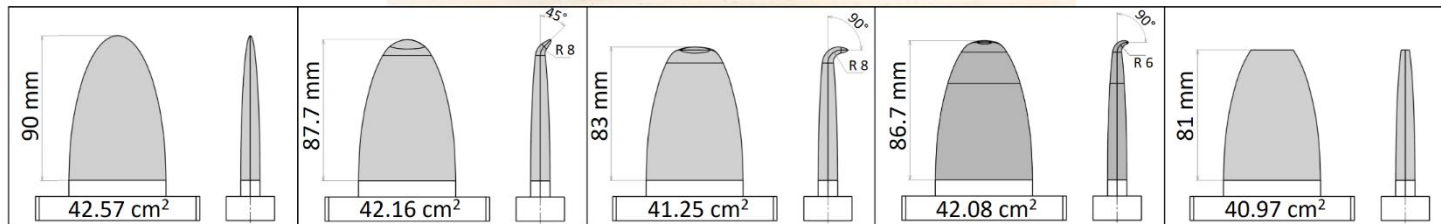
S : span of the baseline hydrofoil (90 mm)

Experimental Setup

Manufactured hydrofoils from bronze



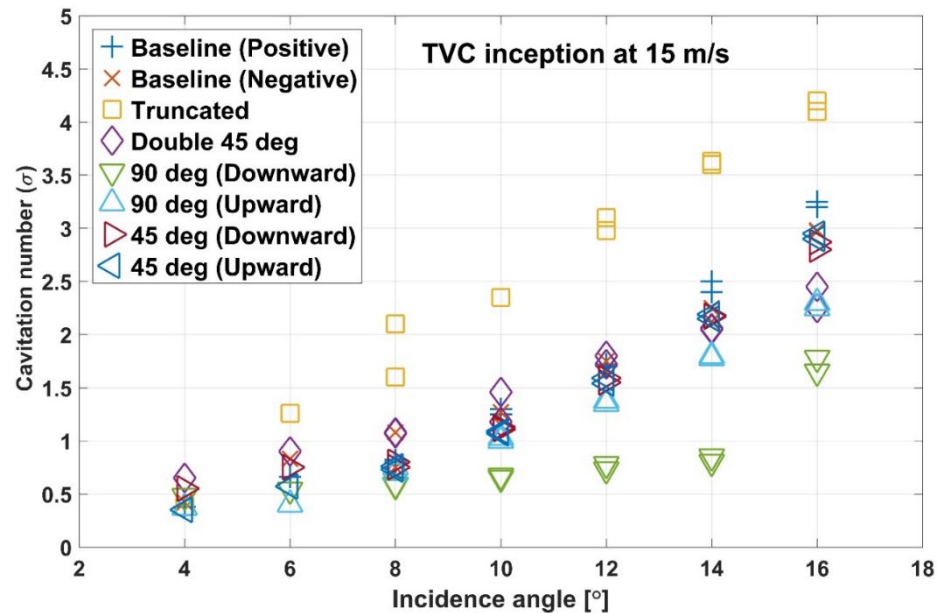
*Upward &
Downward winglets*



TVC inception results

Tests performed at $U_\infty = 15 \text{ m/s}$ and fully saturated water for **10%-bent winglets**.

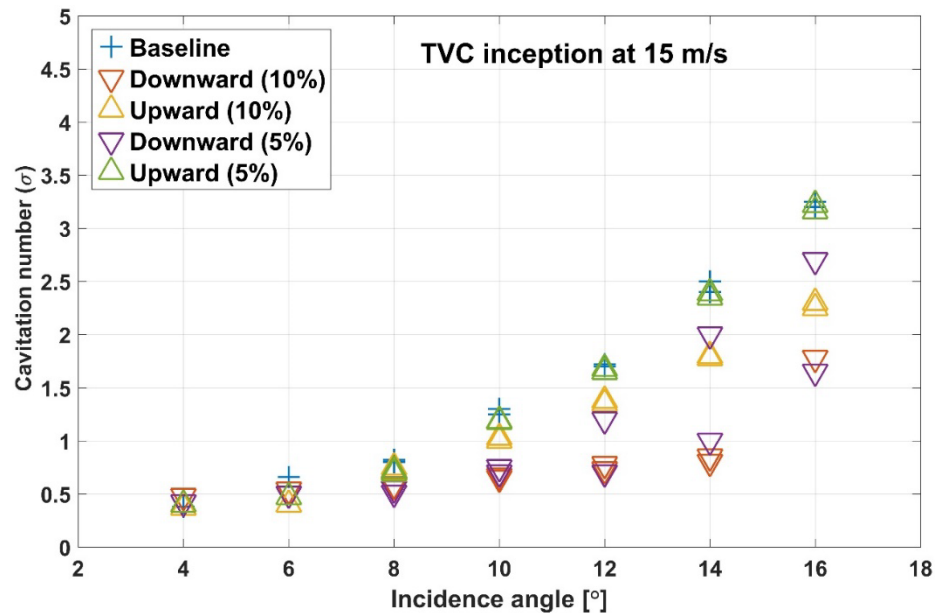
- The **90° winglet bent toward the pressure side** shows an outstanding performance.



TVC inception results

Tests performed at $U_\infty = 15 \text{ m/s}$ and fully saturated water for **10%-bent winglets**.

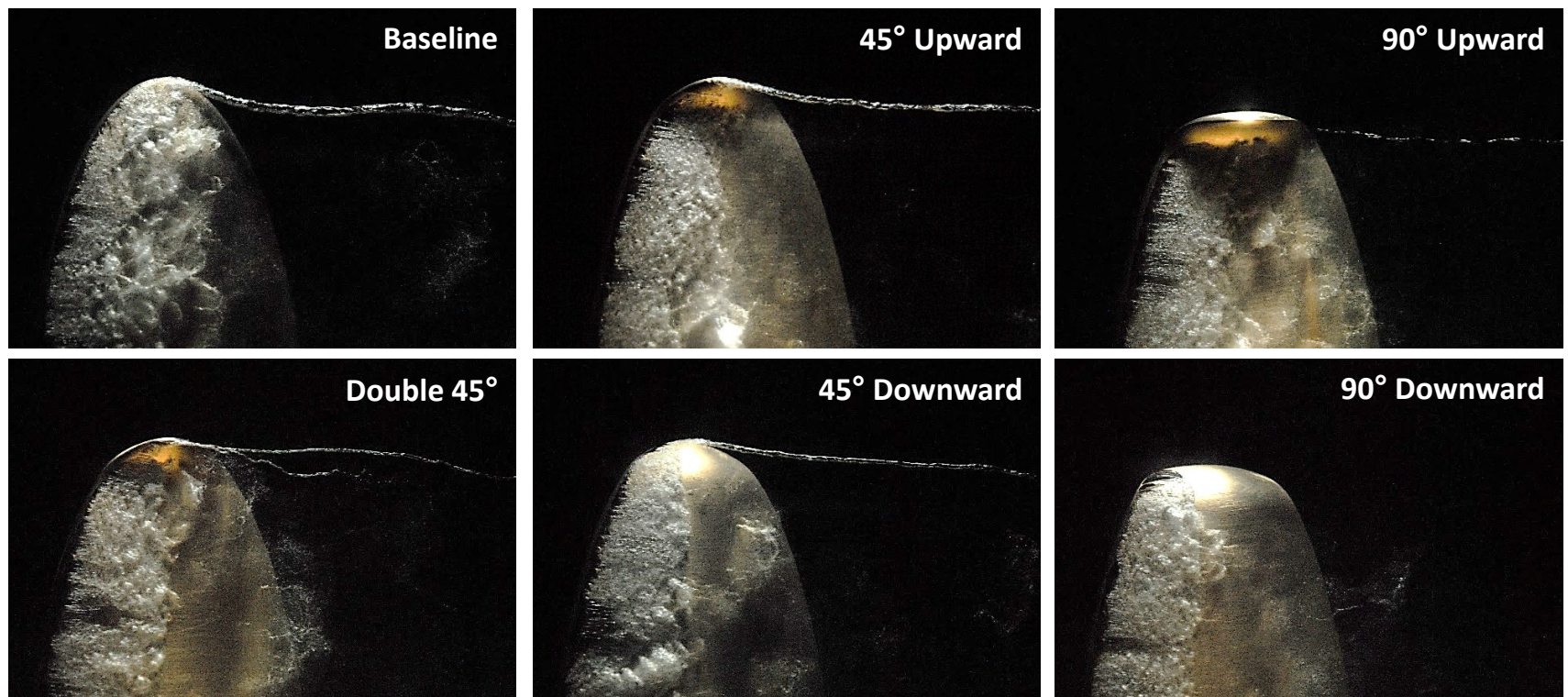
- The **5%-bent** winglets are **less effective** in TVC mitigation.



Flow visualizations

Effect of various winglets on TVC ($Re = 600,000$)

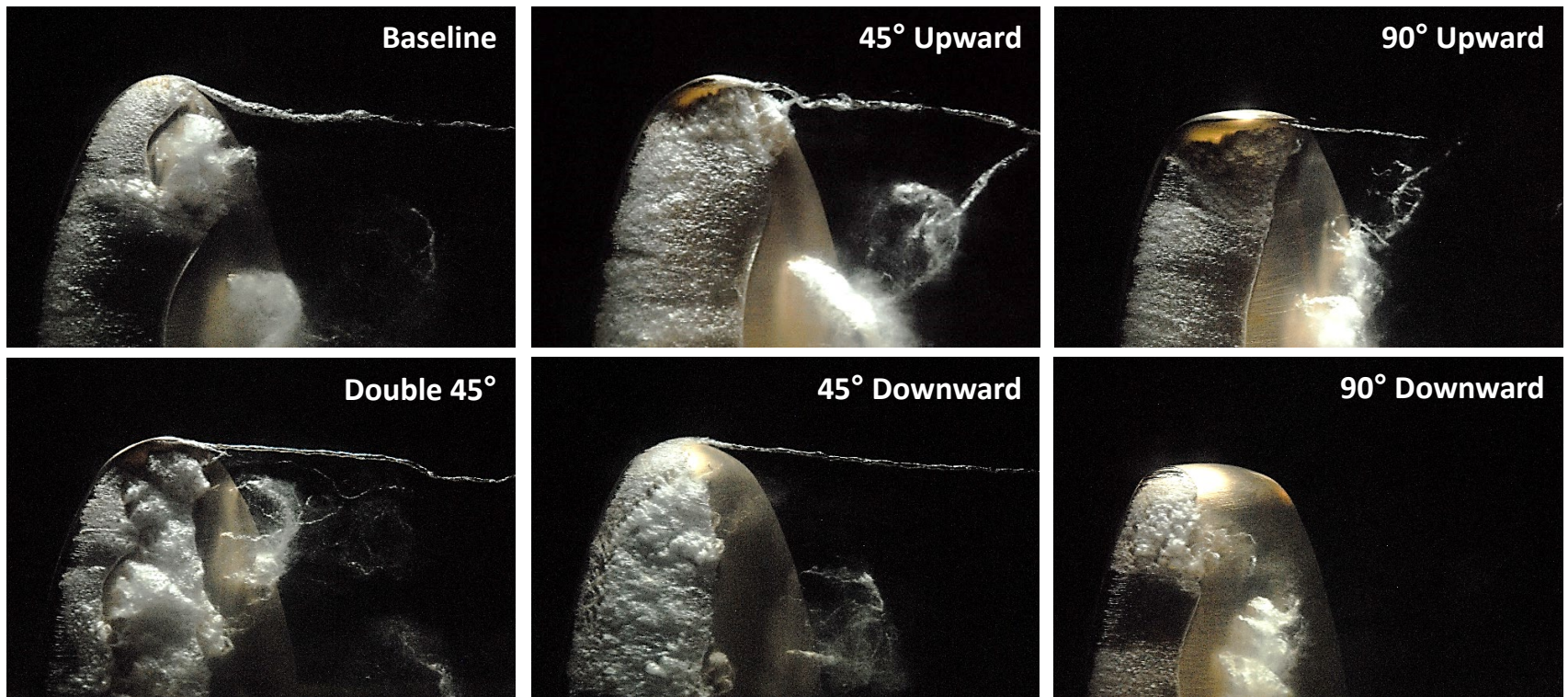
Test conditions: $U_\infty = 10 \text{ m/s}$, $\alpha = 12^\circ$, $\sigma = 1.2$



Flow visualizations

Effect of various winglets on TVC ($Re = 900,000$)

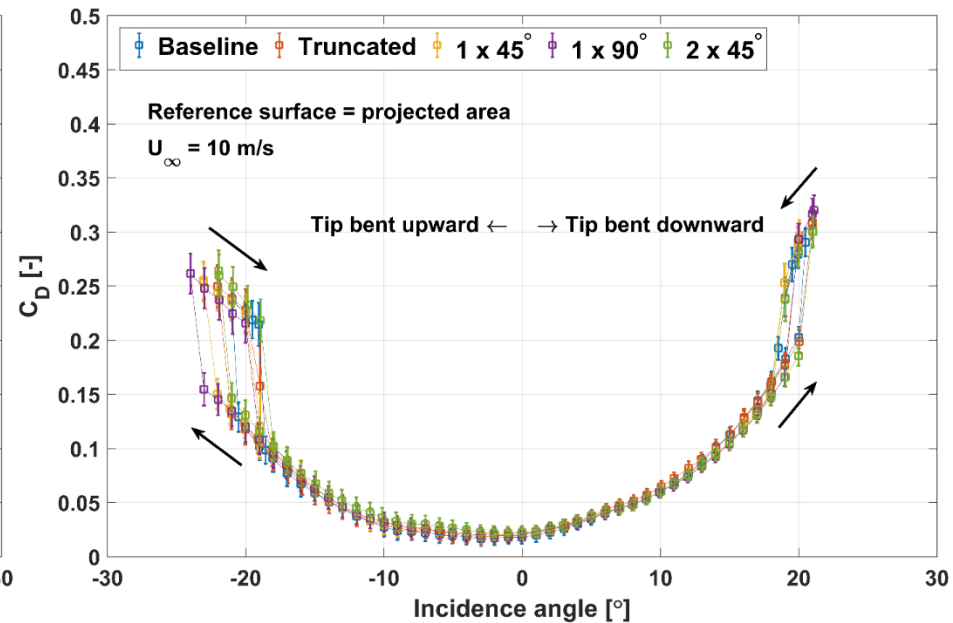
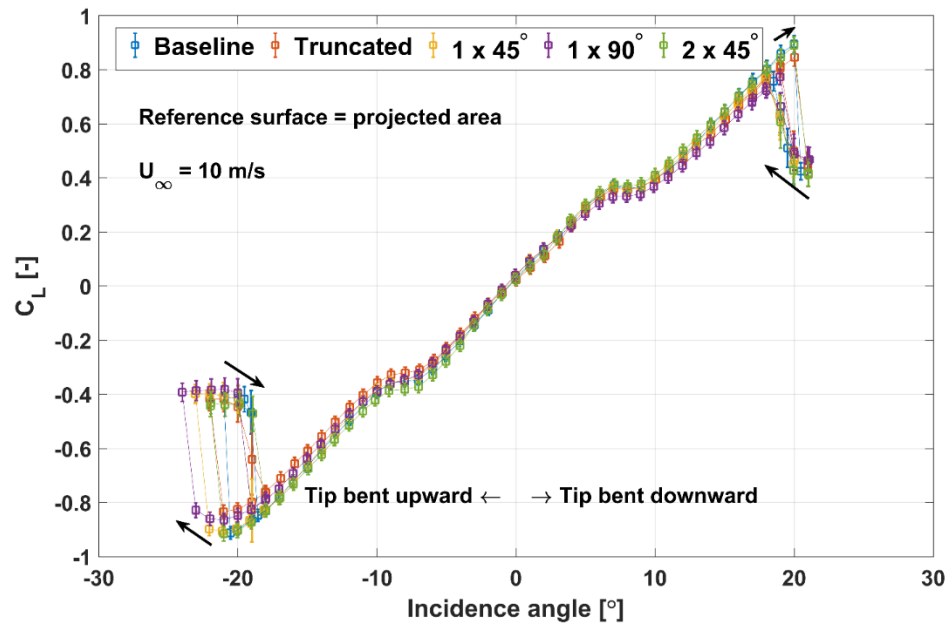
Test conditions: $U_\infty = 15 \text{ m/s}$, $\alpha = 12^\circ$, $\sigma = 1.2$



Lift & drag measurements

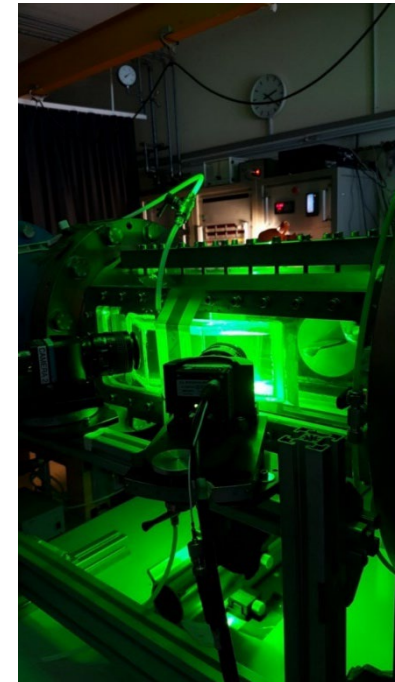
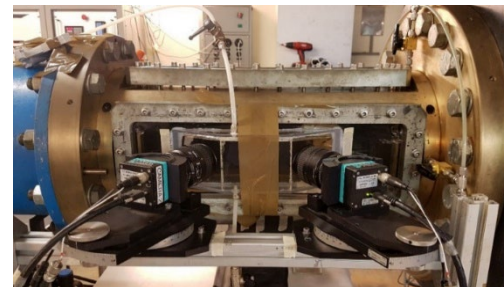
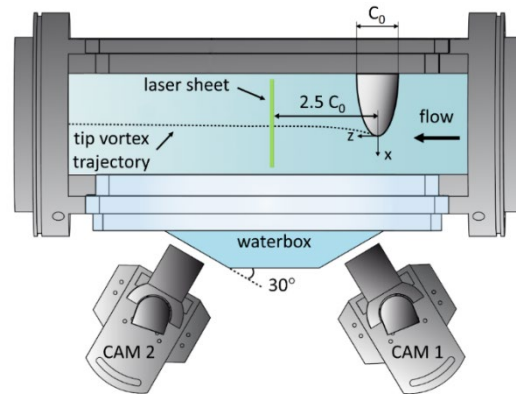
Measurements performed at 10 m/s to avoid cavitation

- Almost **similar** hydrodynamic performances are obtained for all the hydrofoils



Stereo-PIV setup

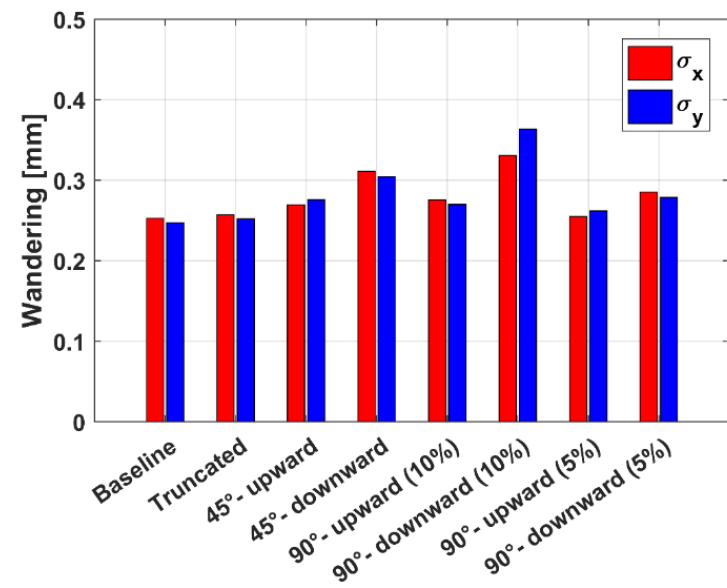
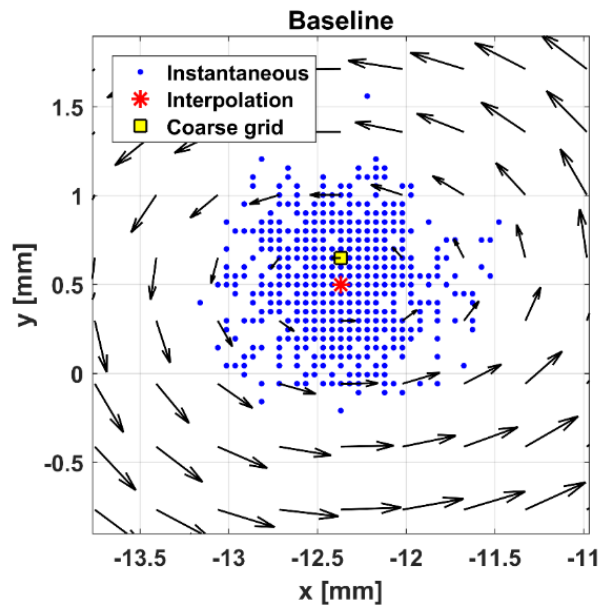
- Double-pulsed laser (135 mJ/pulse)
- Seeding particles
 - Hollow glass spheres
 - Average diameter of $10\ \mu\text{m}$
- 1000 image-pairs for each flow condition
- Vector-to-vector resolution of $0.35\ \text{mm}$
- Wandering motion correction
 - Center detection by Graftieaux algorithm
 - 2D cubic spline interpolation
- Vatistas vortex model curve-fit



Velocimetry Results

Wandering effect and its correction

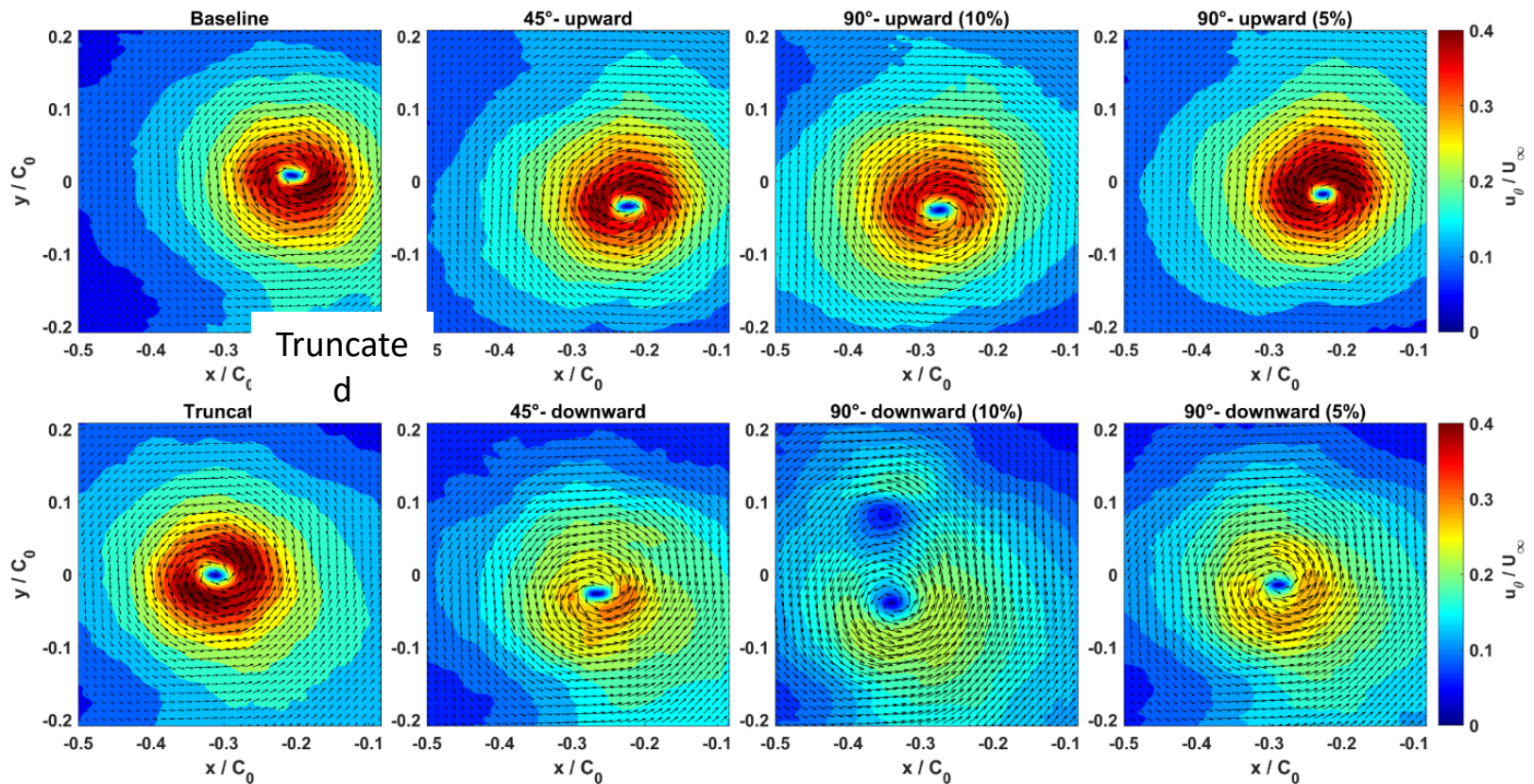
- Flow conditions: $U_{\infty} = 10 \text{ m/s}$, $\alpha = 12^{\circ}$
- 30 - 40% of variations between different hydrofoils
- Higher for downward configurations
- Sub-grid fluctuations



Stereo-PIV results

Contours of the **tangential velocity**

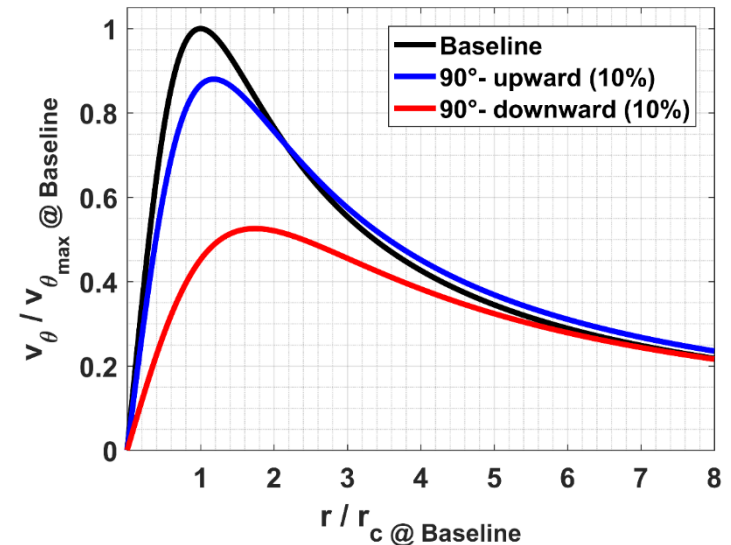
- Flow conditions: $U_\infty = 10 \text{ m/s}$, $\alpha = 12^\circ$



Velocimetry Results

Comparison of the tangential velocity profiles:

- Flow conditions: $U_\infty = 10 \text{ m/s}$, $\alpha = 12^\circ$
- **90°-downward (10%)**
 - Outstanding suppression effects
 - Increasing the viscous radius (r_c) by 70 %
 - Decreasing $v_{\theta_{max}}$ to almost 50 %

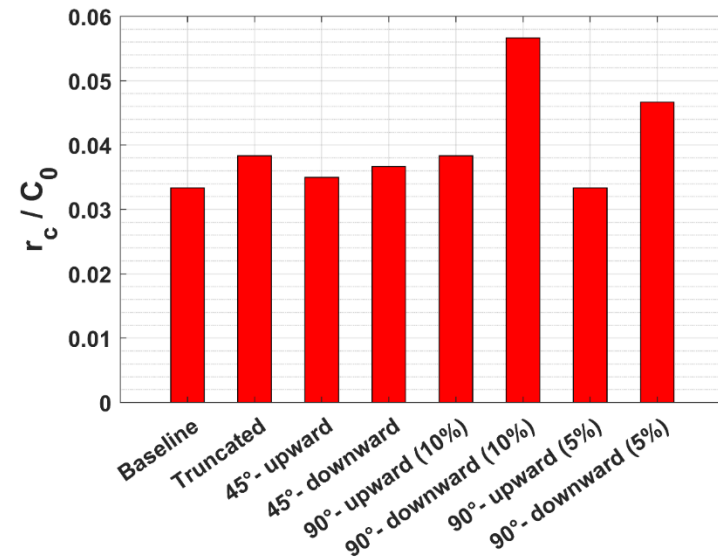
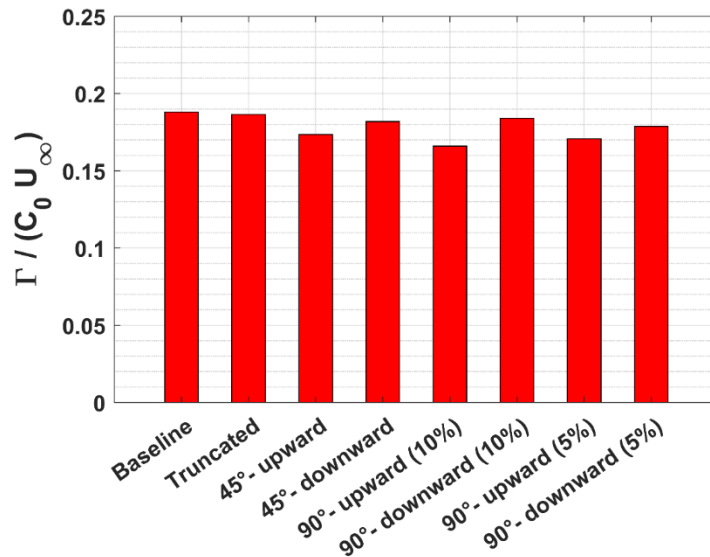


- ✓ Γ remains constant while r_c increases
- ✓ **Viscous core thickening** is the dominant mechanism of TVC mitigation

Velocimetry Results

Comparison of the tangential velocity profiles

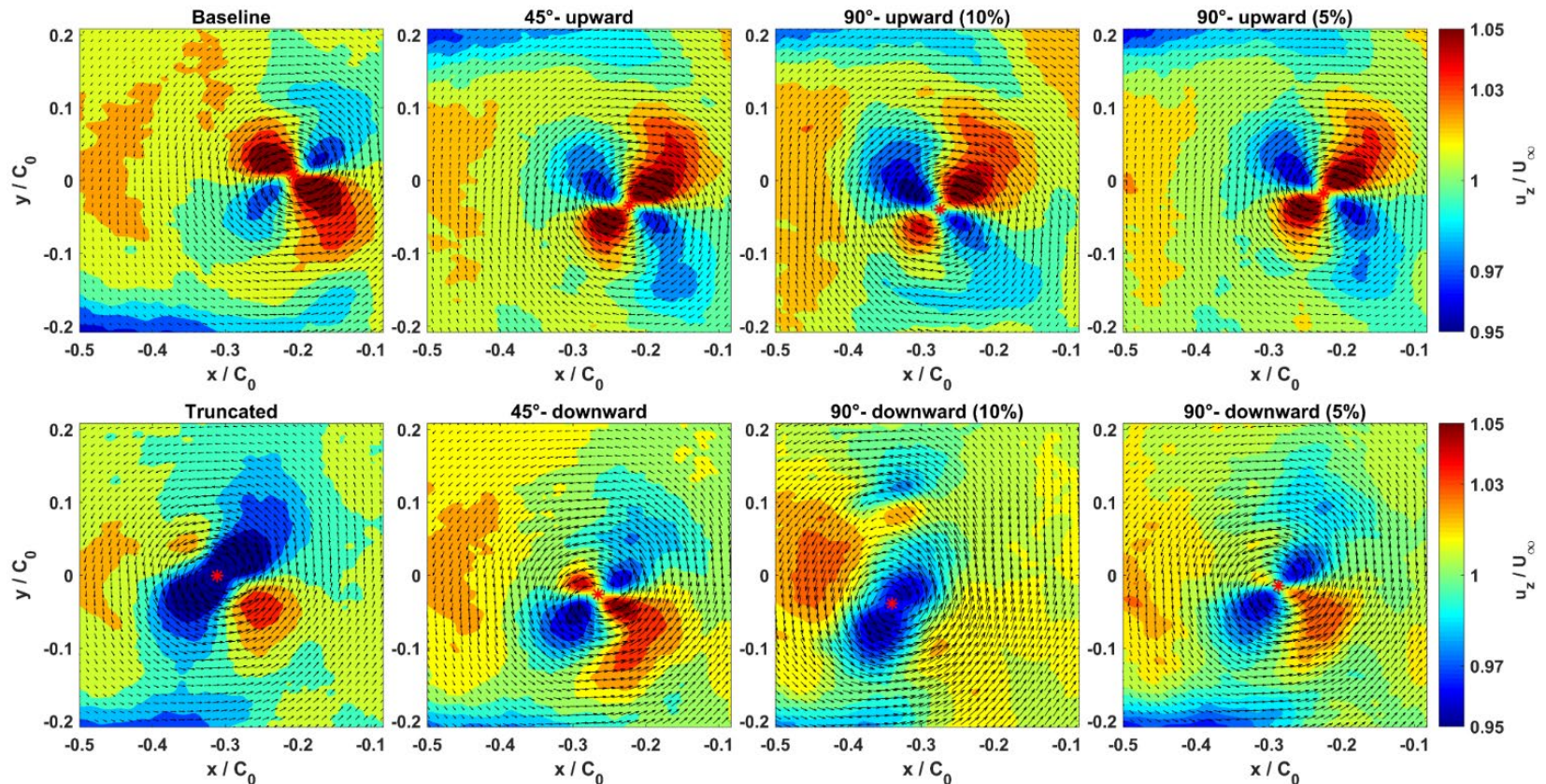
- Same flow conditions: $U_\infty = 10 \text{ m/s}$, $\alpha = 12^\circ$
 - Azimuthally-averaged profiles
- Γ remains constant while r_c increases
- *Viscous core thickening* is the dominant mechanism of TVC mitigation



Velocimetry Results

Contours of the axial velocity

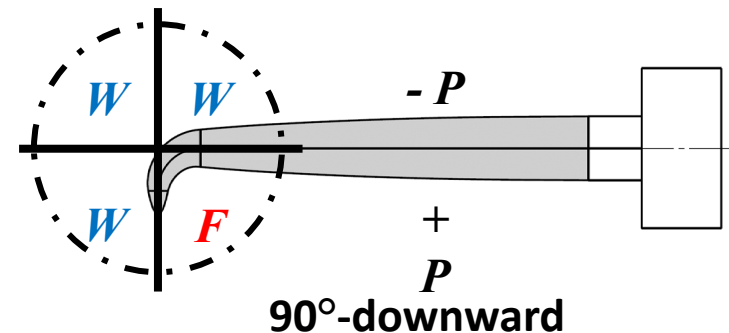
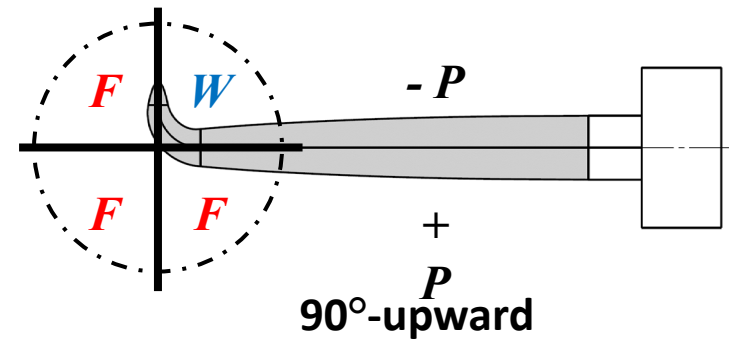
- Flow conditions: $U_\infty = 10 \text{ m/s}$, $\alpha = 12^\circ$



Velocimetry Results: Discussion

The higher effectiveness of the downward configurations is due to the fact that:

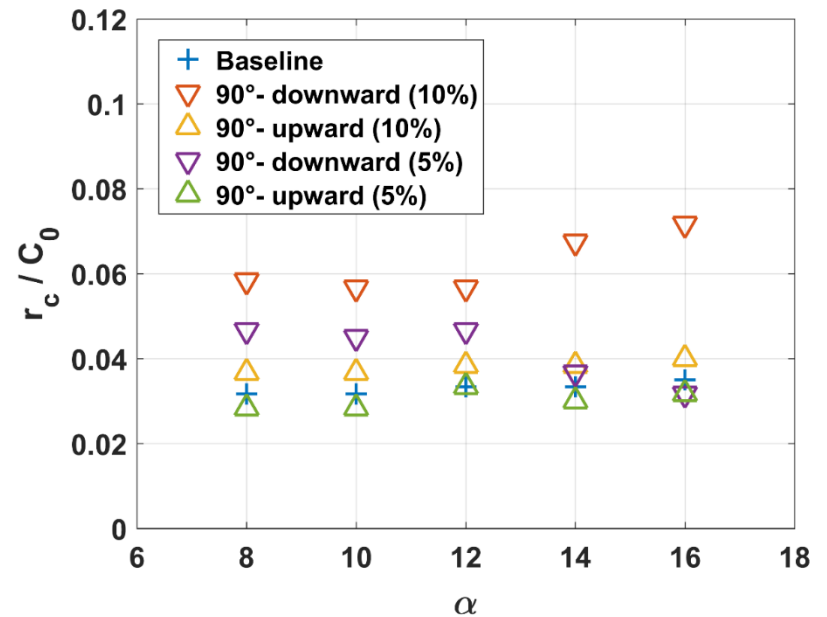
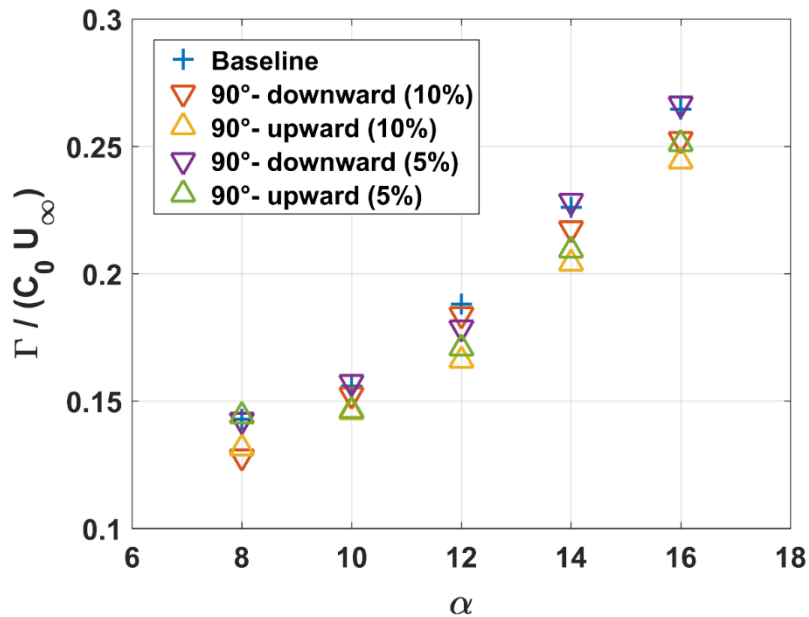
- 1) A downward-facing winglet facilitates the entrainment of the **wake** into the vortex flow,
- 2) which, in turn, increases the momentum diffusion rates, and thereby,
- 3) smooths down the velocity profiles.



Velocimetry Results

Effect of incidence angle on Γ and r_c

- Flow conditions: $U_\infty = 10 \text{ m/s}$
- Similar trends are conserved



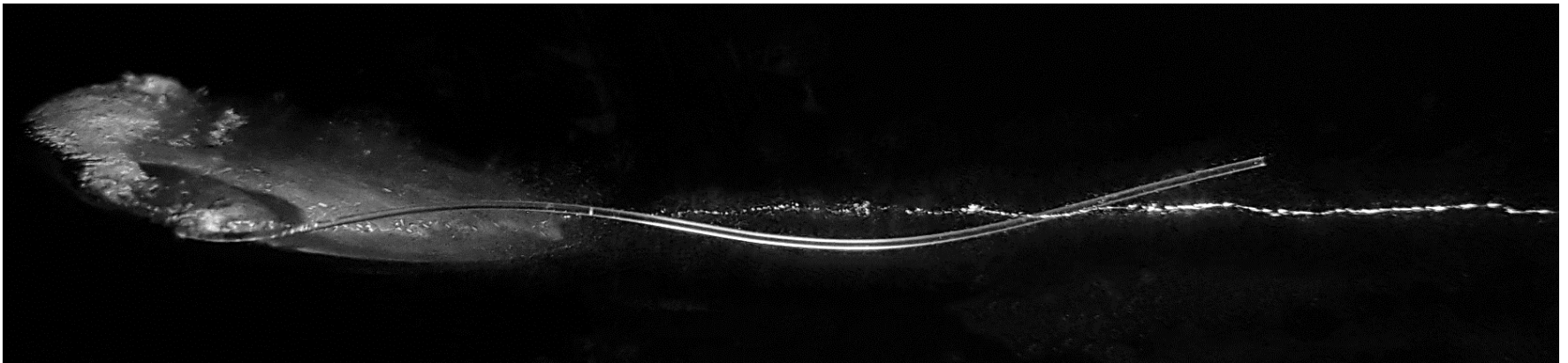
Conclusion



Effectiveness of nonplanar winglets in TVC suppression is investigated:

- Almost for all the flow conditions, the winglet-equipped hydrofoils perform better than the baseline hydrofoil in terms of delaying TVC.
- The hydrodynamic performances of the hydrofoils are **not** degraded by the winglets.
- For $L_{BS} = 0.1S$, $\theta = 90^\circ$ yielded much better results compared to $\theta = 45^\circ$.
- The negative dihedral angles (**downward**) are superior to the positive ones (**upward**), due to enhanced **wake entrainment** effects.
- Longer vertical sections outperform the shorter ones.
- Best configuration performance: **10%-bent 90°-downward**
 - Outstanding suppression (68% delay in inception)
 - Increasing the viscous core radius by 70%
 - Decreasing $v_{\theta_{max}}$ to almost 50%

Mitigating Tip Vortex Cavitation by a Flexible Trailing Thread

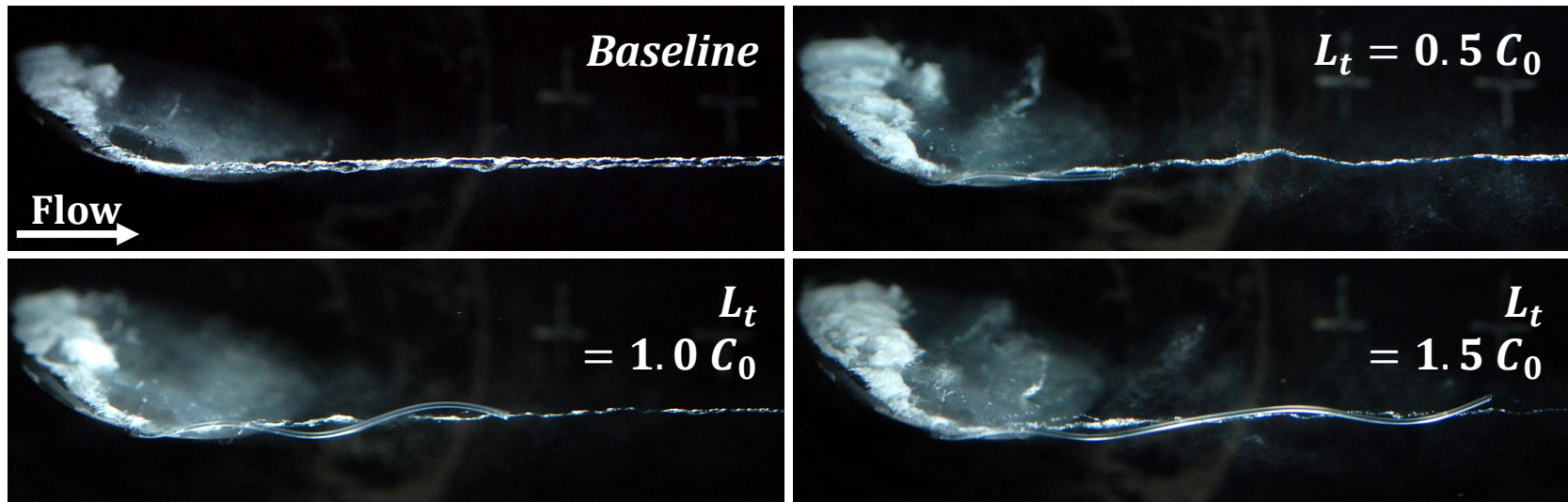


Ali Amini, Jeonghwa Seo, Shin Hyung Rhee, and Mohamed Farhat. "Mitigating tip vortex cavitation by a flexible trailing thread." *Physics of Fluids* 31, no. 12 (2019): 127103.

TVC Suppression Mechanisms

Interaction of a flexible trailing thread with the cavitating vortex flow

- Flow conditions: $\alpha = 15^\circ$, $U_\infty = 15$ m/s, and $\sigma = 1.8$
- Effect of the thread length (L_t) on TVC suppression (thread diameter: $d_t = 0.7$ mm)
- C_0 is the root chord length of the hydrofoil ($C_0 = 60$ mm)



Analysis of the thread motion

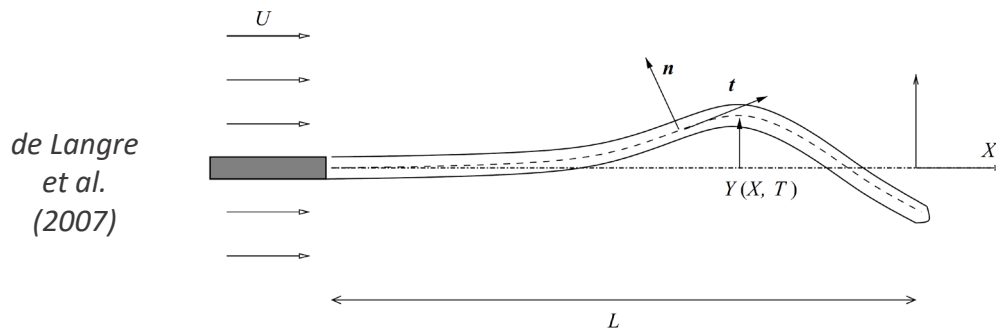
- The most rigid thread tested under the following conditions → **Two stable** states
 - Test conditions: $\alpha = 10^\circ$, $U_\infty = 10$ m/s, $\sigma = 1.2$, $d_t = 0.7$ mm and $L_t = 0.5 C_0$
- Freestream velocity → Acceleration vs Deceleration → Static vs Dynamic response
- The thread should be **flexible enough** to **align** with the vortex and **interact** with it dynamically.

But, what does ***flexible enough*** mean?



Analysis of the thread motion

The lateral motion of a flexible beam retained straight in axial flow is analyzed.



de Langre
et al.
(2007)



Non-dimensional
velocity

$$u = \left(\frac{\rho A}{EI} \right)^{1/2} U_{\infty} L_t$$

flexural
rigidity

$$EI \frac{\partial^4 y}{\partial x^4} - \frac{\partial}{\partial x} \left(\Theta(x) \frac{\partial y}{\partial x} \right) + m \frac{\partial^2 y}{\partial t^2} = F_{fluid}$$

fluid-induced
forces

variation of local
axial tension

Acceleration term
 m : mass per unit length

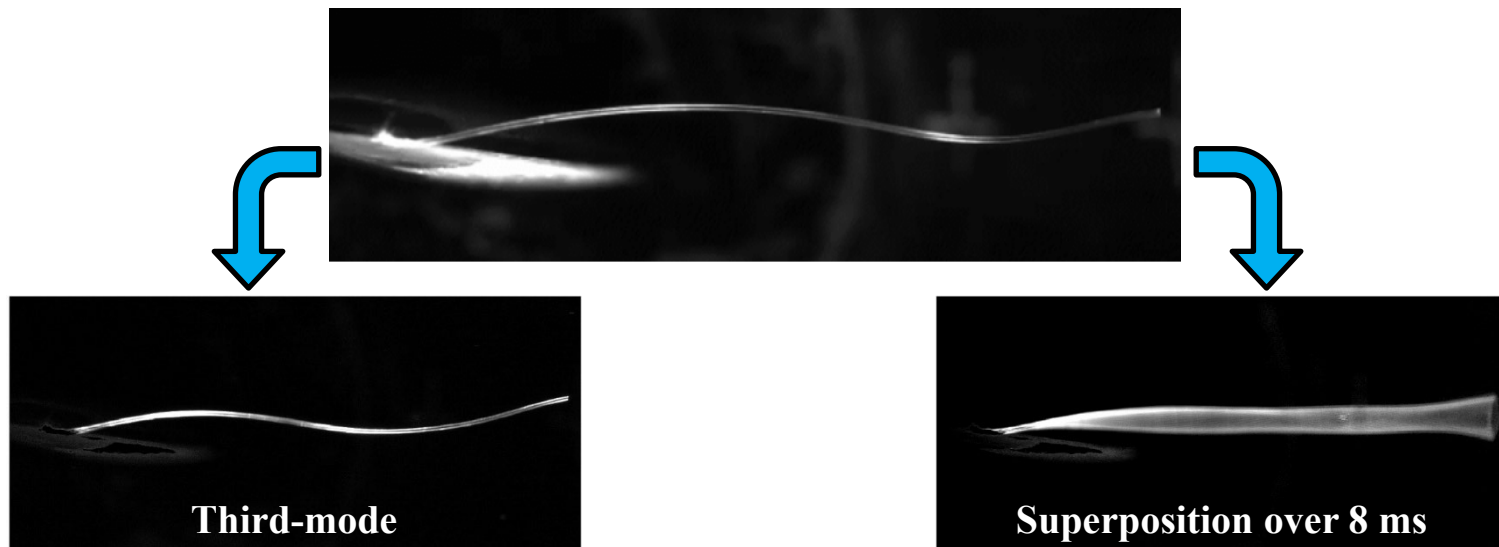
TVC Suppression Mechanisms

➤ Analysis of the thread motion

- Test conditions: $d_t = 0.5$ mm, $L_t = 1.5 C_0$, $\alpha = 10^\circ$ and $U_\infty = 10$ m/s

➤ Harmonic waves are travelling along the thread.

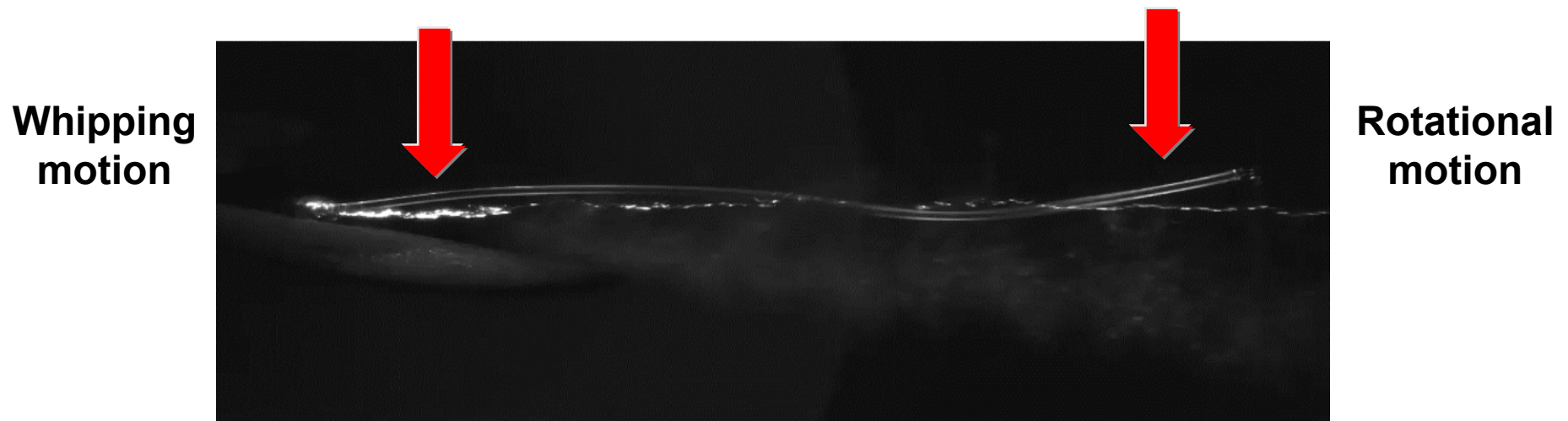
➤ The thread clearly encloses the vortex axis by **rotating** around it.



TVC Suppression Mechanisms

Dynamic interaction of the trailing thread and the vortex flow

- Flow conditions: $\alpha = 12^\circ$, $U_\infty = 10 \text{ m/s}$, and $\sigma = 1.4$
- Thread configuration: $d_t = 7 \text{ mm}$ and $L_t = 1.5 C_0$
- A complex interaction is observed



Analysis of the Whipping Motion

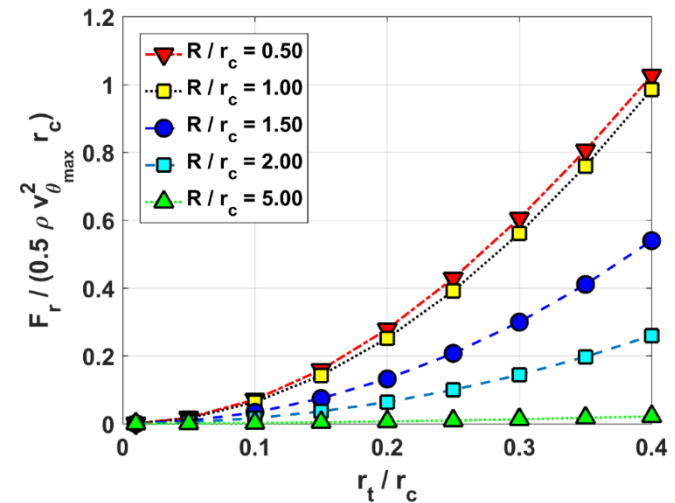
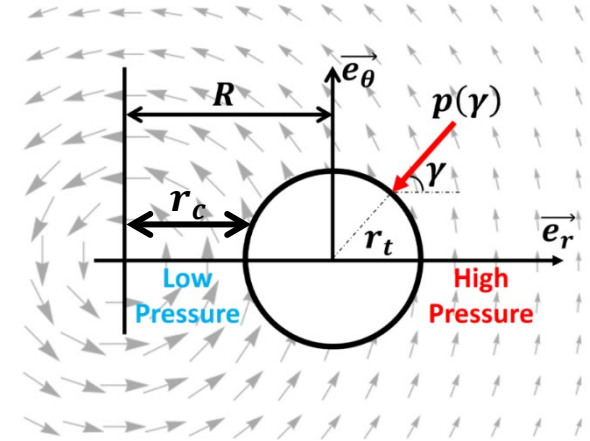
- A Lamb-Oseen vortex profile is considered:

$$v_{\theta}(r) = \frac{\Gamma}{2\pi r} \left(1 - e^{-1.256(r/r_c)^2}\right) \quad \text{and} \quad \frac{\partial p}{\partial r} = \rho \frac{v_{\theta}^2}{r}$$

- Calculating the **attraction force (F_r)** in one-way coupling for various thread diameters and eccentricities results in:

$$F_r = 2r_t \int_0^{\pi} p(\gamma) \cos(\gamma) d\gamma$$

- The radial force increases with the thread diameter, **however**, this increase becomes more significant as the thread gets closer and closer to the vortex axis.
- Away from the vortex axis, the relation is almost linear.
- Close to the axis $\rightarrow F_r \propto d_t^2$



Analysis of the Whipping Motion

Modeling of the coincidence phase:

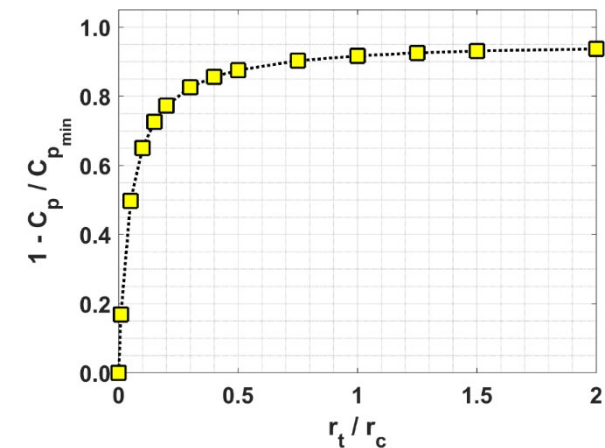
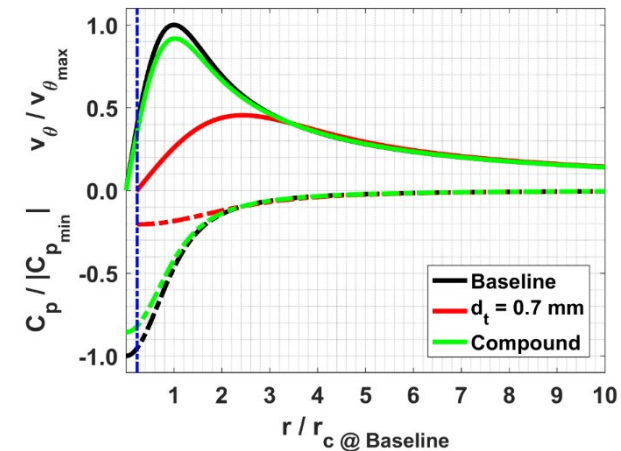
- The coincidence phase is **fast**, which implies that the **integral parameters** of the vortex should remain constant. ($\Gamma_1 = \Gamma_2 = \Gamma$)
- To find the **new** viscous core radius, we implement the conservation of angular momentum principle:

$$H_1 = \rho L \Gamma \int_0^{\infty} r \left(1 - e^{-1.256(r/r_c)^2} \right) dr$$

$$H_2 = \rho L \Gamma \int_0^{\infty} \frac{r^2}{r - r_t} \left(1 - e^{-1.256((r-r_t)/r_{c,2})^2} \right) dr$$

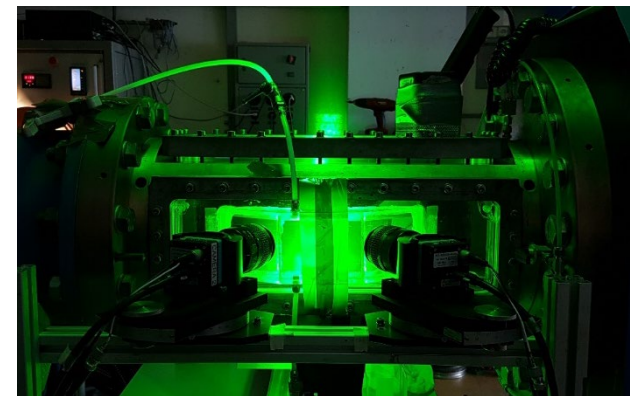
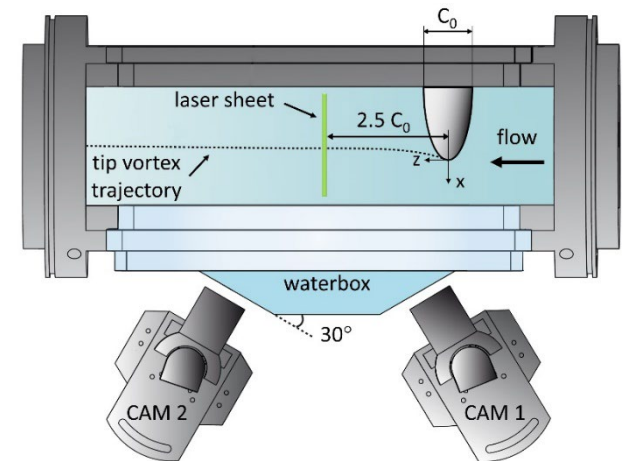
- The coincidence of the thread results in a considerable rise in the minimum pressure induced by the vortex.
- The pressure rise is almost proportional to $r_t^{0.2}$

Arbitrary Lamb-Oseen vortex
with $r_c = 1.5$ mm



Stereo-PIV setup

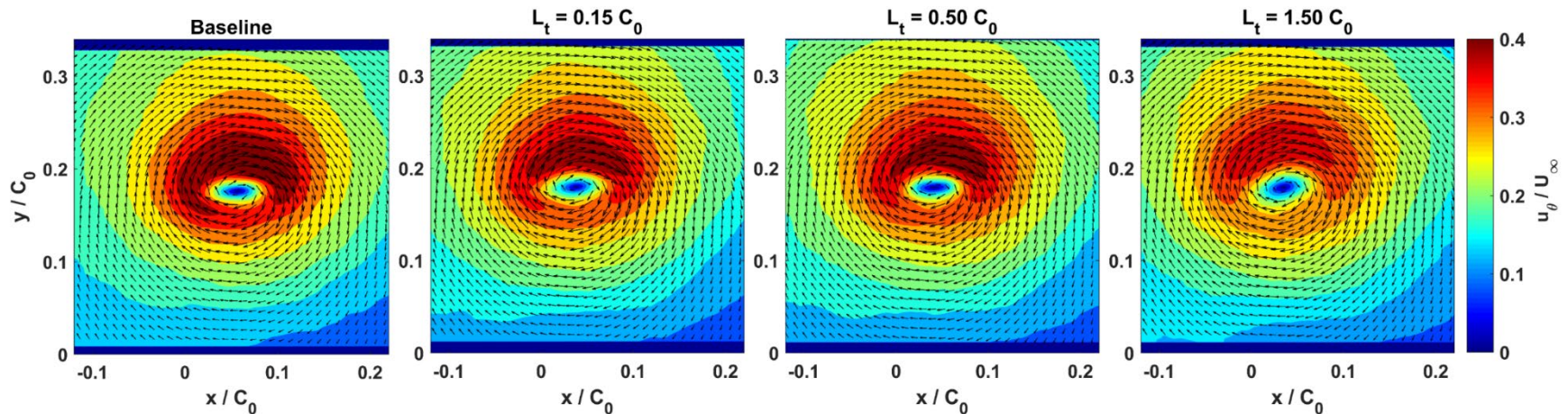
- Double-pulsed laser (135 mJ/pulse)
- Seeding particles
 - Hollow glass spheres
 - Average diameter of 10 μm
- 1000 image-pairs for each flow condition
- Vector-to-vector resolution of $0.3 \times 0.4 \text{ mm}$
- Wandering motion correction
 - Center detection by Graftieaux algorithm
 - 2D cubic spline interpolation
- Vatisas vortex model curve-fit



Velocity measurements

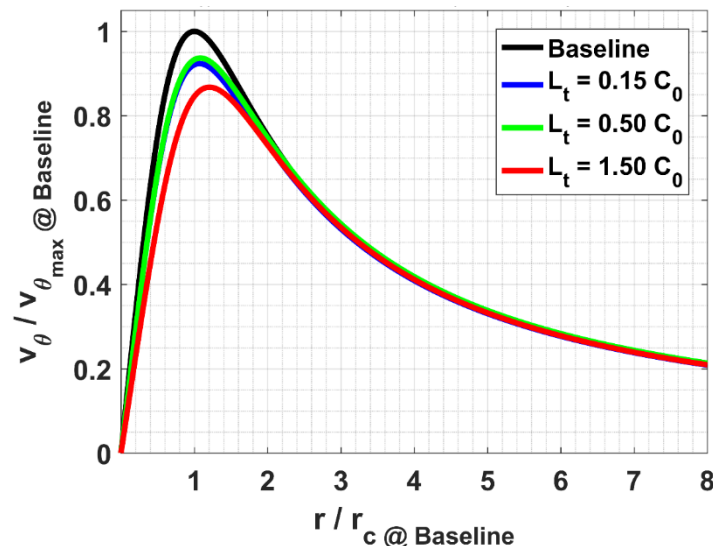
Contours of the **tangential** velocity:

- Flow conditions: $U_\infty = 10 \text{ m/s}$, $\alpha = 12^\circ$
- Thread configuration: $d_t = 0.7 \text{ mm}$
- A clear **reduction** is observed in the magnitude of the tangential velocity.



Azimuthally-averaged v_θ profiles

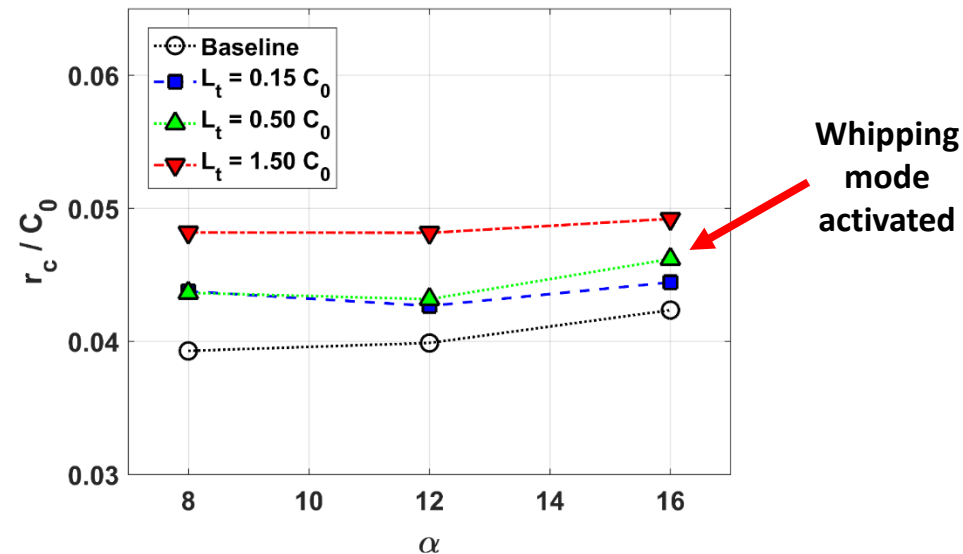
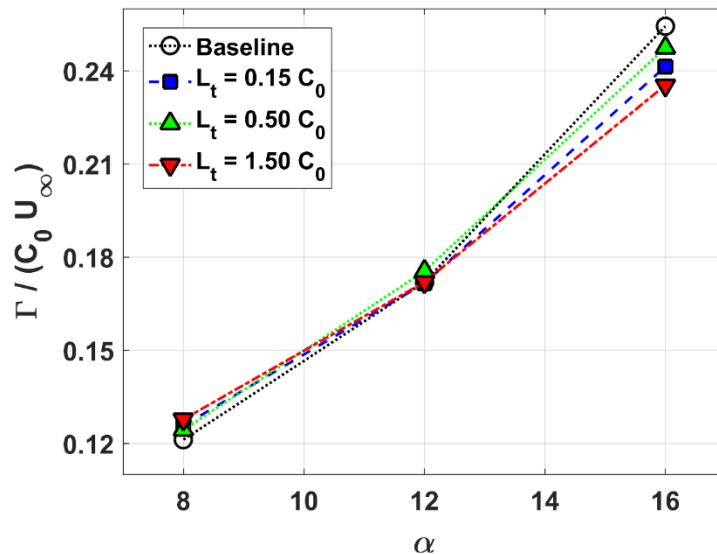
- Test conditions: $\alpha = 12^\circ$, $U_\infty = 10 \text{ m/s}$ and $d_t = 0.7 \text{ mm}$.
- A clear **reduction** is observed in the magnitude of the tangential velocity.
- In this test, $L_t = 0.5 C_0$ is in **non-flapping** state.
 - The **winglet effect** for the rigid structures implies the **augmented turbulent mixing**.



Velocity measurements

Effect of *incidence angle* on tip vortex parameters at various thread lengths.

- Flow conditions: $U_\infty = 10 \text{ m/s}$ and non-cavitating regime
- Vortex intensity is conserved and TVC suppression is due to a **viscous core thickening**.



Discussion:

Now, let's put all the **effective parameters** together:

- The extent of thread-vortex interaction $\rightarrow u = \left(\frac{\rho A}{EI}\right)^{1/2} U_\infty L_t$
- The likelihood of whipping motion $\rightarrow F_r \propto d_t^2$
- The pressure rise due to the whipping $\rightarrow \Delta p \propto d_t^{0.2}$

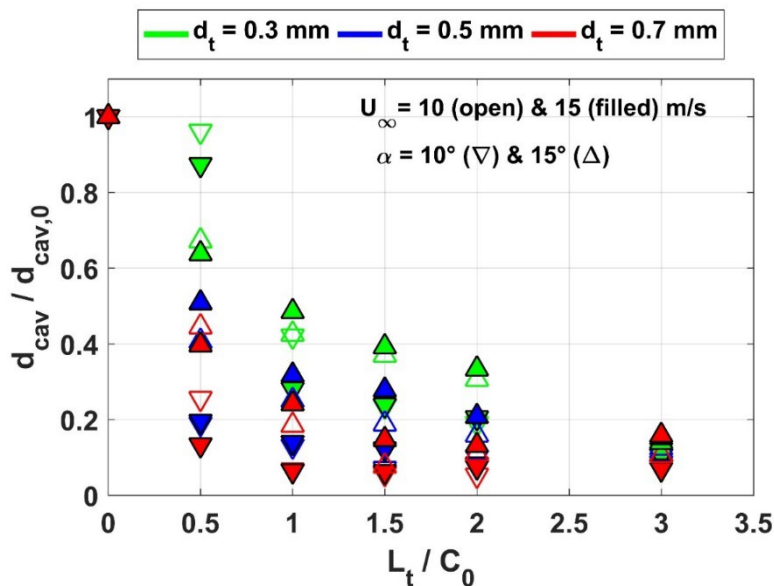
➤ If we multiply the three terms together and scale the **thread diameter** with the **viscous core radius**, we get the following non-dimensional variable:

$$L^* = \frac{4}{r_c^{2.2}} \sqrt{\frac{\rho}{E}} U_\infty L_t d_t^{1.2}$$

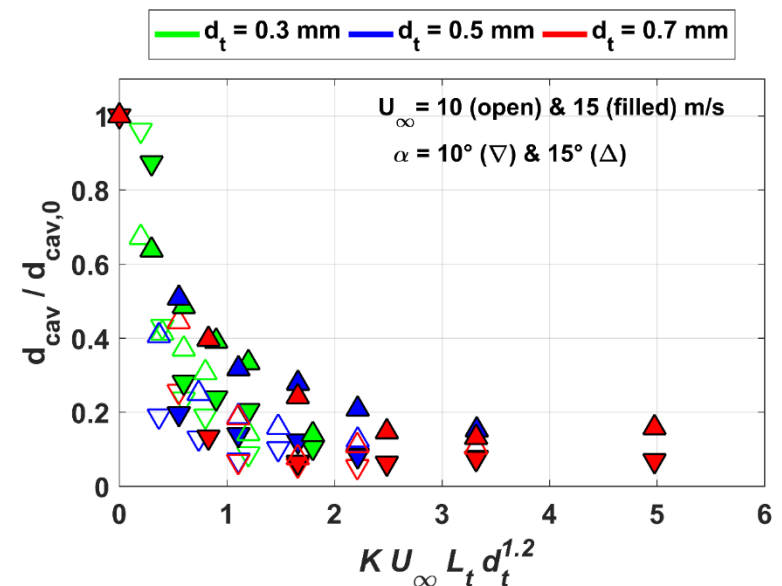
Discussion:

Plotting TVC suppression against the non-dimensional variable:

- The suppression effect is saturated beyond $L^* \cong 2$ for all the configurations.



$$K = \frac{4}{r_c^{2.2}} \sqrt{\frac{\rho}{E}}$$



Conclusion

Effectiveness of a flexible thread in TVC mitigation

- A thread should be **flexible enough** to:
 - Get ***aligned*** with the vortex
 - Interact with it ***dynamically***
- **Two interaction/mitigation regimes:**
 - ***Rotational*** motion
 - ***Whipping*** motion
- **Viscous core thickening**

